Bitlis Eren Üniversitesi Fen Bilimleri Dergisi
BİTLİS EREN UNIVERSITY JOURNAL OF SCIENCE
ISSN: 2147-3129/e-ISSN: 2147-3188
VOLUME: 12 NO: 4 PAGE: 1069-1082 YEAR: 2023
DOI:10.17798/bitlisfen.1328893

Assessing the Effects of Water Content on the Unconfined Compression Strength of Egg White-Stabilized Khorasan Mortar

Emrah DAĞLI[1], Murat ÇAVUŞLU[1*]

[1]*Zonguldak Bulent Ecevit University, Civil Engineering, Zonguldak, Türkiye*
(ORCID: 0000-0002-5744-8151) (ORCID: 0000-0002-2285-8513)

Keywords: Brick ballast, Egg white, Khorasan mortar, Lime, Sand, Unconfined compression strength.

Abstract

Khorasan mortar, a traditional, durable, and environmentally friendly building material, has been utilized for centuries in the Khorasan region of Türkiye. Its composition, which is based on natural hydraulic lime, imparts exceptional strength, breathability, and workability, making it suitable for diverse construction projects. Consequently, investigating the mechanical properties of Khorasan mortar, specifically its interaction with stone elements in historical buildings, in various mixing ratios, can provide valuable insights into the preservation and future of these architectural treasures. This study focuses on researching Khorasan mortar as a material of interest, utilizing brick ballast, lime, standard sand, water, and egg white, with a particular emphasis on egg white-stabilized Khorasan mortar. Four different water contents (70%, 80%, 90%, and 100%) were carefully selected, based on the dry mass of the egg white, to prepare a total of 12 samples (three identical samples for each water content) for testing. Prior to testing, the samples were cured for seven days in a desiccator. Unconfined compression strength tests were conducted, and axial strain-stress graphs were plotted to determine the unconfined compression strength (UCS) of the mixtures. The results revealed that the mixtures containing 80% water content exhibited the highest UCS values, while the samples with 90% and 100% water content demonstrated similar UCS values. The minimum UCS was approximately 0.518 times the maximum value, suggesting the importance of optimizing the water amount in Khorasan mortar formulations.

1. Introduction

The preservation of cultural heritage stands as a powerful testament to a nation's strength, with the imperative for enduring structures resonating across the globe. This demand has compelled engineers to explore and investigate materials that can withstand the pressures exerted on buildings, emerging as a significant global concern. Khorasan mortar, historically employed in civil engineering structures by various empires such as the Ottoman, Roman, Byzantine, and Seljuk [1], epitomizes a traditional mortar that has thrived for centuries in the Khorasan region of Türkiye, encompassing present-day Iran, Afghanistan, and Central Asia. Celebrated for its exceptional durability, strength, and distinctive composition, Khorasan mortar relies primarily on natural hydraulic lime (NHL) or hydraulic lime derived from quicklime obtained by burning limestone with clayey impurities. The utilization of NHL endows the mortar with the ability to set and harden even in the presence of moisture, rendering it particularly suitable for construction in humid or wet environments. A fundamental hallmark of Khorasan mortar lies in its dependence on natural materials and sustainable production methods, effectively reducing the environmental impact associated with the production of conventional Portland cement-based mortars. This alignment corresponds with the mounting global emphasis on eco-friendly and sustainable building practices. Furthermore,

*Corresponding author: murat.cavusli@beun.edu.tr
Received: 17.07.2023, Accepted: 23.09.2023

Khorasan mortar offers several practical advantages. Its exceptional breathability facilitates the efficient transfer of moisture vapor, mitigating the risk of trapped moisture within the masonry. This attribute holds particular value for historic restoration projects and regions with high humidity, averting damage caused by moisture accumulation. Moreover, Khorasan mortar showcases superior workability and adhesion properties, empowering skilled craftsmen to achieve intricate and precise detailing in masonry construction, while its flexibility accommodates the natural movements of buildings, diminishing the likelihood of cracks or structural damage. Overall, Khorasan mortar represents a sustainable and high-performance alternative to conventional mortars, rendering it a favored choice for a wide spectrum of construction projects, spanning from the preservation of historical landmarks to contemporary sustainable architecture. The recent devastating earthquakes that struck the southeastern part of Türkiye brought the use of Khorasan mortar to the forefront once again. Historical structures constructed with this mortar have proven their resilience due to the strength conferred by lime [1]. Notably, Khorasan mortar exhibits remarkable resistance to seawater, making it highly suitable for cities in close proximity to the seaside, where moisture content is substantial. Various studies have examined the usage of different admixtures in Khorasan mortar [2-9]. For instance, egg white can be incorporated in a mixture at a ratio between 5% and 25%, with 10% appearing to be the optimum ratio in terms of maintaining strength [2]. The addition of polypropylene fiber admixture reduces mortar shrinkage by approximately 35% compared to control samples [3]. The investigation of lime/aggregate and lime/brick aggregate ratios revealed that a 1:1 ratio yielded the maximum compressive strength [4]. Calcium-rich fly ashes prove effective in mixtures due to their significant CaO content. When fly ash was added to the mixture, along with tile ballast, at varying ratios (10%, 20%, 30%, and 40%), compressive strength was notably enhanced by up to 75% [7]. The optimization of lime/aggregate and lime/brick aggregate ratios in Khorasan mortar demonstrated that ratios of 0.67 and 0.75, respectively, yielded the best results [8]. Additionally, the inclusion of a low percentage (between 2.5 and 10) of bentonite improved the unconfined compression strength (UCS) of the mortar, with 5% being the optimum ratio, resulting in an approximate 20% enhancement in UCS values [9]. The extended setting time and relatively lower strength of Khorasan mortar in comparison to cement can be addressed by modifying additives or adjusting water content in the mortar. Canbaz and Güler [11] examined the effect of lime type on the properties of Khorasan mortar. According to analysis results, they revealed that lime type had significant effects on the strength of Khorasan mortar. In this study, the effect of water content on the unconfined compression strength value was investigated, with egg white serving as an additive. The water content of any mixture containing clayey materials can provide insights into its strength and durability. Given the paucity of research on this subject, this study aims to contribute to the body of knowledge surrounding Khorasan mortar.

2. Material and Method

2.1. General Information

This section provides a comprehensive account of the experimental investigation conducted on Khorasan mortar, delving into the effects of varying water contents. The materials employed in the study comprised brick ballast, lime, and standard sand, all derived from the Khorasan clay. These materials were procured from Ekşioğlu Ltd. Şti., a local company located in the center of Zonguldak. Additionally, eggs were obtained from a local market. Brick ballast was used as a powder form. Fig. 1 illustrates all the materials utilized in the study, which were stored in a controlled room environment devoid of any direct exposure to sunlight. During the preparation of Khorasan mortar, the materials were mixed with the help of a special tray at certain mixing ratios until they became homogeneous. The chemical compositions of materials were presented in Table 1. Then, the aggregate gradations were shown in Figs. 2-4

Figure 1. Materials used for the Khorasan mortar a) brick ballast b) standard sand c) lime d) egg white.

Table 1. The chemical composition of materials

Chemical composition (%)	SiO_2	Al_2O_3	Fe_2O_3	TiO_2	CaO	MgO	K_2O	Na_2O	SO_3	Free CaO	L.O.I.	Water Absorption Rate (%)
Brick ballast	62.1	17.9	10.31	0.38	1.46	1.41	1.93	NA	0.03	NA	10.2	14
Lime	1.51	1.63	0.76	NA	91.90	2.55	0.18	NA	1.26	NA	NA	13
Powder	98.03	NA	NA	NA	1.15	NA	NA	NA	NA	NA	NA	2.8

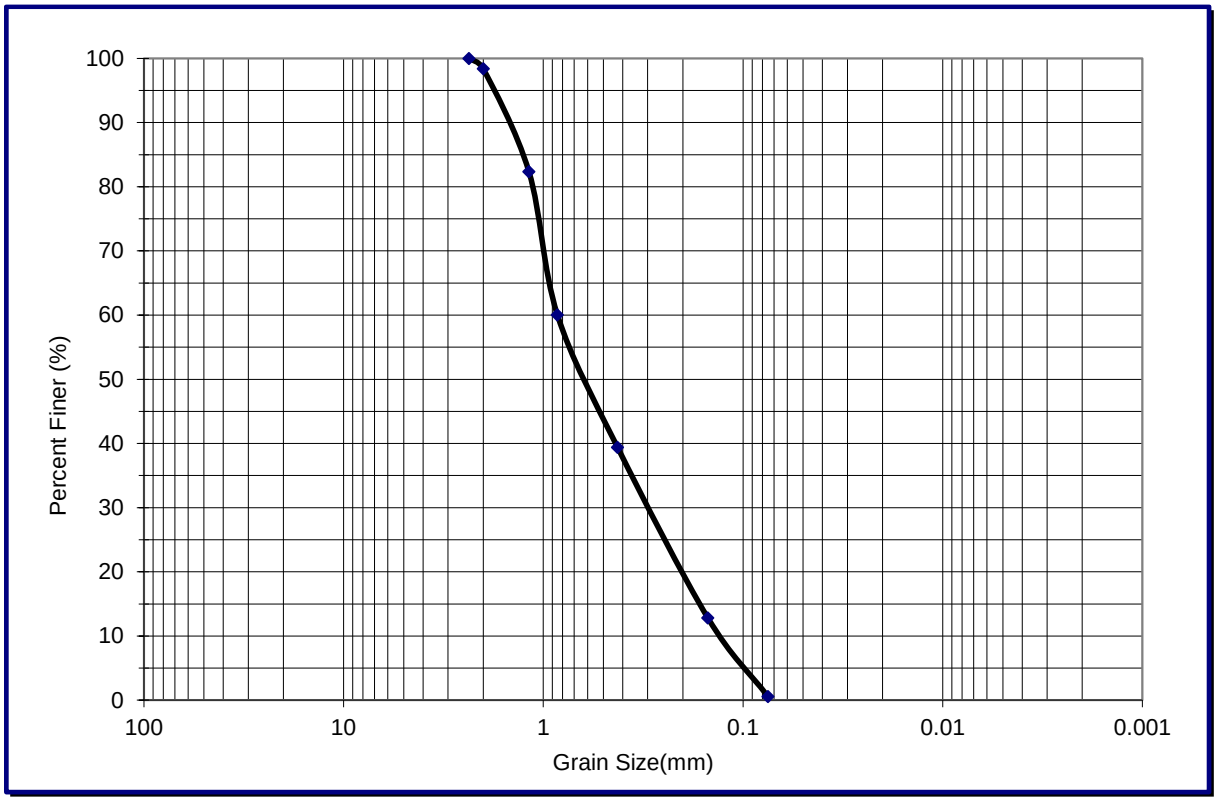

Figure 2. The aggregate gradation of sand.

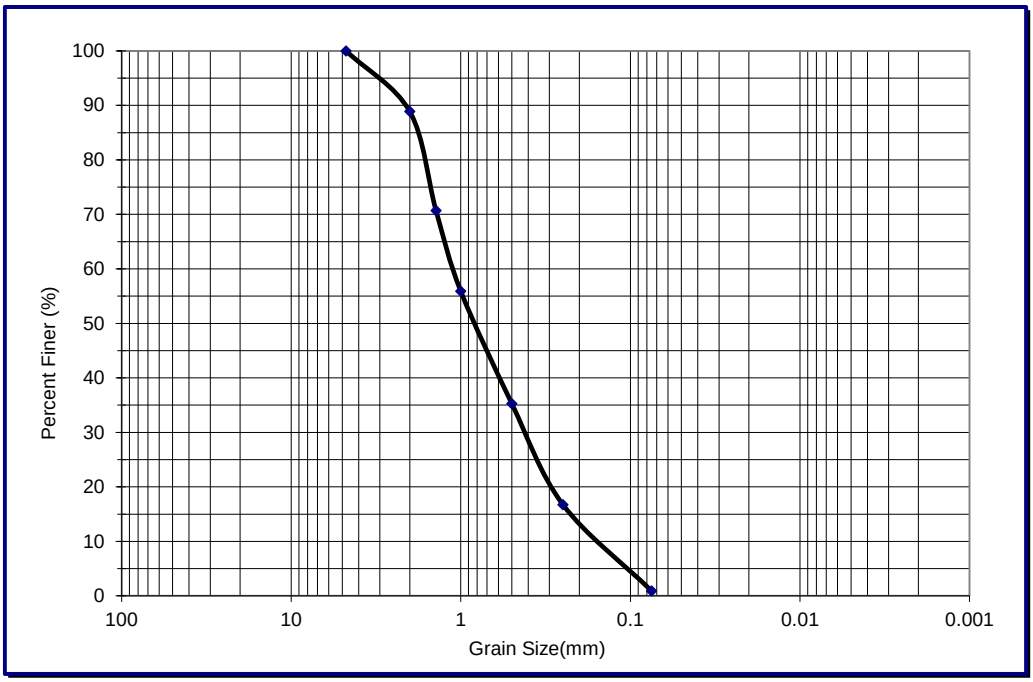

Figure 3. The aggregate gradation of brick ballast.

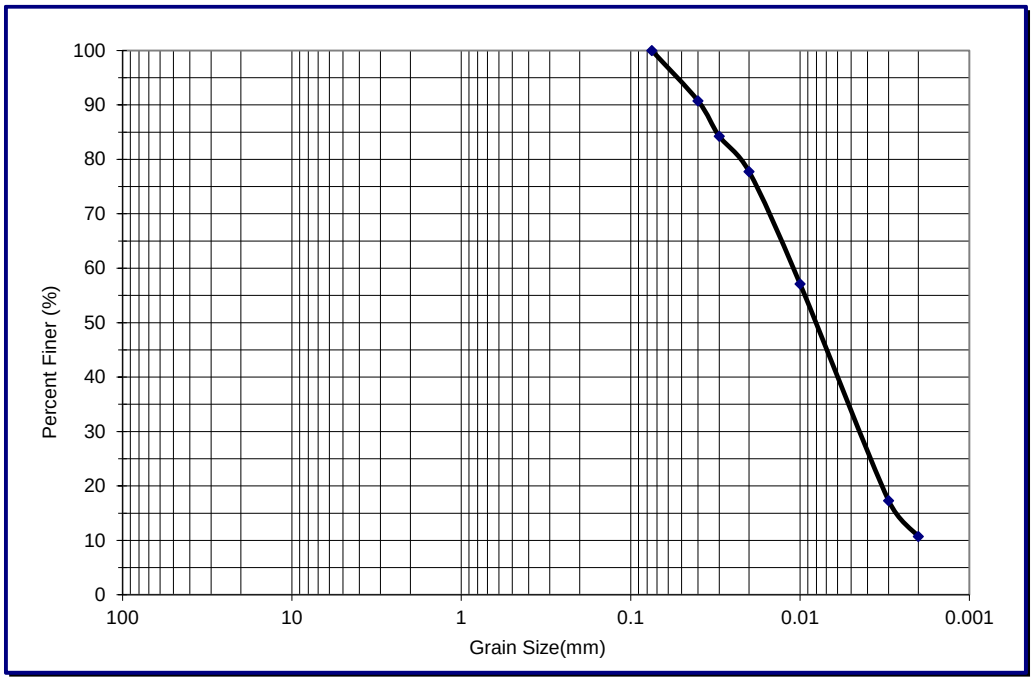

Figure 4. The aggregate gradation of lime.

This study encompassed the utilization of four different water content levels, namely 70%, 80%, 90%, and 100%. The determination of water content was based on the formula "water amount * 100/egg white," thereby expressing the water percentage relative to the dry mass of the egg white. For each water content level, three identical samples were meticulously prepared, ensuring consistency in both water amount and additive quantity. The primary constituents of Khorasan mortar, namely brick ballast, standard sand, and lime, were combined in a ratio of 9:3:4, respectively, within the mixture. Notably, a 60% water content level was initially attempted numerous times; however, the samples

proved fragile and lacked cohesion during preparation, leading to their exclusion from the study. To facilitate better comprehension, the mixtures were assigned unique codes. For instance, the mixture code EW70C7-1 signifies "EW" as egg white, "70" representing the water percentage relative to the egg white amount, "S" denoting the sample, and "1" indicating the sample number. There were prepared 3 identical (same additive ratio and same water content) samples. Therefore, samples were numbered as 1, 2 and 3. The admixture ratio within the mixture mirrors that of the lime component. Further details regarding the mixture compositions can be found in Table 2.

Table 1. Mixture details

Mixture Code	Sample Number	Water (g)	Egg White (g)	Brick Ballast (g)	Standard Sand (g)	Lime (g)
EW70S1	1	28	40	90	30	40
EW70S2	2	28	40	90	30	40
EW70S3	3	28	40	90	30	40
EW80S1	1	32	40	90	30	40
EW80S2	2	32	40	90	30	40
EW80S3	3	32	40	90	30	40
EW90S1	1	36	40	90	30	40
EW90S2	2	36	40	90	30	40
EW90S3	3	36	40	90	30	40
EW100S1	1	40	40	90	30	40
EW100S2	2	40	40	90	30	40
EW100S3	3	40	40	90	30	40

2.2. Specimen Preparation

Brick ballast was prepared for use by grinding it with a Los Angeles abrasion test device. A total of 1500 revolutions were performed to attain a finer material suitable for testing purposes. Additionally, egg white was exclusively incorporated after being broken and mixed in a porcelain dish. The materials comprising Khorasan mortar were meticulously blended to ensure homogeneity. To achieve smooth and uniform compaction, equal amounts of the sample were poured for each layer. The compaction process was carried out using specialized Harvard compaction test equipment, as illustrated in Fig. 5a.

a) b) c)

Figure 5. Harvard test equipment **a)** full set **b)** compaction mould **c)** compaction with hammer.

2.2. Unconfined Compression Strength (UCS) Test

Unconfined compression strength test is one of the most important signs of the change in strength and it is not a time-consuming test. Usage of low number of materials (because of the preparation of test with Harvard miniature compaction test equipment) make this test also favorable. There is no study that research the unconfined compression strength of Khorasan mortar stabilized soils with various water content. ASTM D2166D2160M-16 [10] standard was used for unconfined compression strength. The cured samples were carefully positioned on an automated triaxial

compression test device, as depicted in Fig. 6. Pertinent information regarding each sample, such as diameter, height, and mixture code, was recorded during the initial stage. A data saving interval of 1 data point per second was selected for precise data acquisition. The approximate dimensions of the samples were measured to be approximately 33 mm in diameter and 71 mm in height.

Figure 6. Automated triaxial compression test device for unconfined compression strength.

To ensure compliance with the standard requirements [10], a loading rate of 0.71 mm/min was selected, as this would facilitate the attainment of a 10% axial strain within a 10-minute duration of the test. The lower part of the device was gradually elevated until it made contact with the sample, while the top part was positioned accordingly. The efficacy of this alignment was verified by monitoring the load variation displayed on the program screen. The automated triaxial compression test device provided comprehensive results pertaining to the axial stress and strain of the samples.

3. Results and Discussion

This section provides a concise summary of the stress-strain graphs obtained from the automated triaxial compression test device for the various mixtures. For instance, in the case of the EW70S1 sample (Fig 7a), the unconfined compression strength (UCS) is determined to be 606.26 kPa, with the axial strain (ε) reaching a value of 2.95% at the maximum stress (UCS). The stress increase during the first 60 seconds of the test (ε = 0 - 1) for the EW70S1 sample was relatively slow, followed by a rapid enhancement beyond ε = 1% until the maximum stress was attained. Similar stress-axial strain behavior is observed for the EW70S2 and EW70S3 samples, as evident from Fig 7b and 7c. The axial strain (ε) values at the maximum stress are found to be closely distributed between 2.23% and 3.02%. The maximum UCS value being 1.13 times the minimum UCS value is within an expected range. The average UCS of the three samples is determined to be 646.88 kPa, which closely aligns with the value of the third sample (EW70S3). Regarding failure behavior, EW70S1 and EW70S3 exhibit similarities, as illustrated in Fig 8a and 8c, while EW70S2 showcases a slightly different failure pattern. The failure image of EW70S2 presents a characteristic 45° angle from the top of the sample to the peak, which is further validated by the axial strain-stress graph in Fig 8b

The EW80S1 sample exhibits an unconfined compression strength (UCS) of 792.33 kPa, with an ε value of 2.42% at the maximum stress, as depicted in Fig. 9a. During the initial 30 seconds of the test (ε = 0 – 0.5) for the EW80S1 sample, stress enhancement was relatively gradual, followed by a rapid increase between ε = 0.5% and 1%. The graph slope exhibited a slower rate during the axial strain range of 1% to 1.5% compared to the first part. The speed of the graph for the third segment, from ε = 1.5% to 2.42%, resembled the behavior observed in the initial part. Notably, the graph behavior for the EW80S1 sample differs slightly from that of EW80S2 and EW80S3, as illustrated in Fig. 9b and 6c. The axial strain (ε) values at the maximum stress are closely distributed between 2.03% and 3.02%. The difference between the maximum and minimum UCS values is 119.63 kPa, which is considered acceptable for this level of UCS, as one value is only 1.15 times that of the other. The average UCS of the three samples is determined to be 853.98 kPa, closely aligning with the value of the second sample (EW80S2). Regarding failure behavior, EW80S1 and EW80S2 demonstrate similarities when observed in Figs. 10a and 10b. Conversely, EW80S3 exhibits failure initiation from the bottom part, while the other samples fail from the top. EW80S2 exhibits a well-known failure pattern characterized by a 45° angle. The axial strain-stress graph in Fig. 10b further supports this observation, as a rapid stress reduction is observed after reaching the UCS value compared to the other samples.

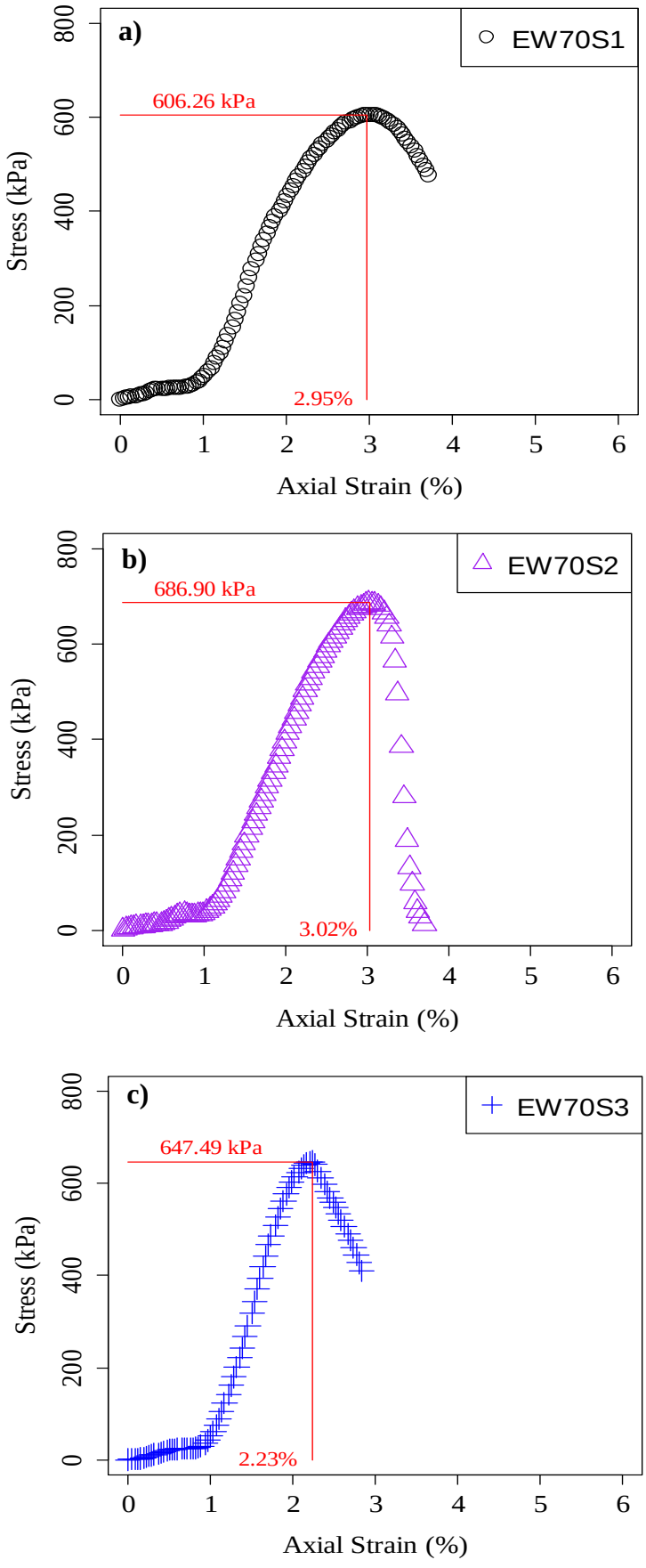

Figure 7. Stress-axial strain graphs for mixtures having 70% water content.

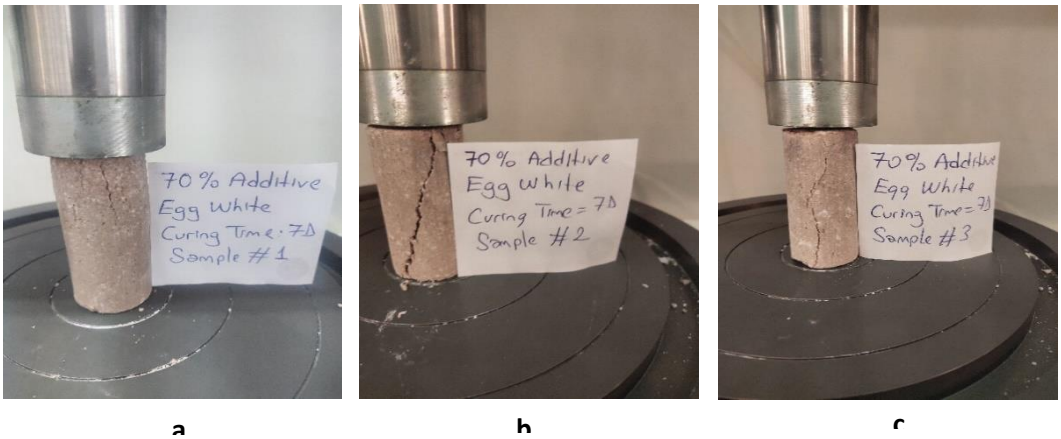

Figure 8. Failure views for samples **a)** EW70S1 **b)** EW70S2 **c)** EW70S3.

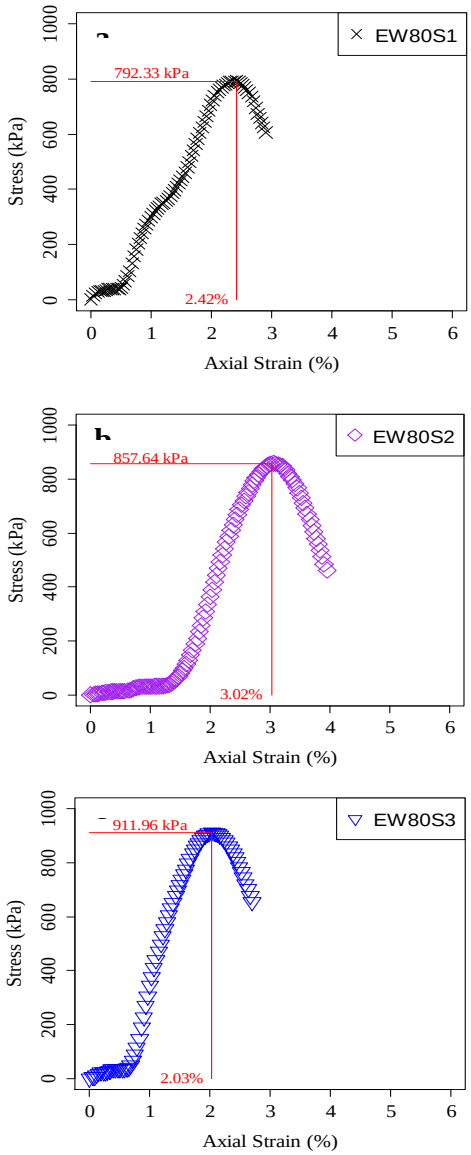

Figure 9. Stress-axial strain graphs for mixtures having 80% water content.

a) **b)** **c)**

Figure 10. Failure views for samples **a)** EW80S1 **b)** EW80S2 **c)** EW80S3.

The EW90S1 sample exhibits an unconfined compression strength (UCS) of 792.33 kPa, with an ε value of 2.42% at the maximum stress, as depicted in Fig. 9a. During the initial 30 seconds of the test (ε = 0 – 0.5) for the EW80S1 sample, stress enhancement was relatively gradual, followed by a rapid increase between ε = 0.5% and 1%. The graph slope exhibited a slower rate during the axial strain range of 1% to 1.5% compared to the first part. The speed of the graph for the third segment, from ε = 1.5% to 2.42%, resembled the behavior observed in the initial part. Notably, the graph behavior for the EW80S1 sample differs slightly from that of EW80S2 and EW80S3, as illustrated in Fig. 9b and 6c. The axial strain (ε) values at the maximum stress are closely distributed between 2.03% and 3.02%. The difference between the maximum and minimum UCS values is 119.63 kPa, which is considered acceptable for this level of UCS, as one value is only 1.15 times that of the other. The average UCS of the three samples is determined to be 853.98 kPa, closely aligning with the value of the second sample (EW80S2). Regarding failure behavior, EW80S1 and EW80S2 demonstrate similarities when observed in Figs. 10a and 10b. Conversely, EW80S3 exhibits failure initiation from the bottom part, while the other samples fail from the top. EW80S2 exhibits a well-known failure pattern characterized by a 45° angle. The axial strain-stress graph in Fig. 10b further supports this observation, as a rapid stress reduction is observed after reaching the UCS value compared to the other samples. The unconfined compression strength (UCS) of the EW90S1 sample is determined to be 516.78 kPa, with an ε value of 2.42% at the maximum stress, as illustrated in Fig. 11a. During the initial 45 seconds of the test (ε = 0 – 0.75) for the EW90S1 sample, stress enhancement was relatively gradual, followed by a rapid increase between ε = 0.75% and 2.42%. The behavior of the second graph for the EW90S2 sample differs from that of EW90S1 and EW90S3, as evident in Figs. 11a, 11b, and 11c. The graphs for EW90S1 and EW90S3 indicate ductile behavior, whereas the graph for EW90S2 exhibits brittle behavior. After reaching the maximum stress, there is a rapid reduction in stress for the EW90S2 sample compared to the graphs of EW90S1 and EW90S3. The axial strain (ε) values at the maximum stress exhibit slight variations between the samples, ranging from 2.42% to 4.65%. The difference between the maximum and minimum UCS values is 89.56 kPa, which is considered acceptable given that one value is only 1.21 times that of the other. The average UCS of the three samples is determined to be 465.18 kPa, which is close to the value of the second sample (EW90S2). Regarding failure behavior, all samples exhibit distinct characteristics when observed in Figs. 12a, 12b, and 12c. The EW90S1 sample appears to be nearly split in half (Fig 12a), while the axial strain-stress graph indicates a ductile behavior. EW90S2 showcases a similar failure pattern (Fig 12b), with a sharp decrease in stress after reaching the maximum value, as observed in Fig. 12b. The bottom part of the EW90S3 sample is observed to have undergone significant breakage, as depicted in Fig. 12c, with a stress value of approximately 380 kPa even when the ε value reaches 6.25%.

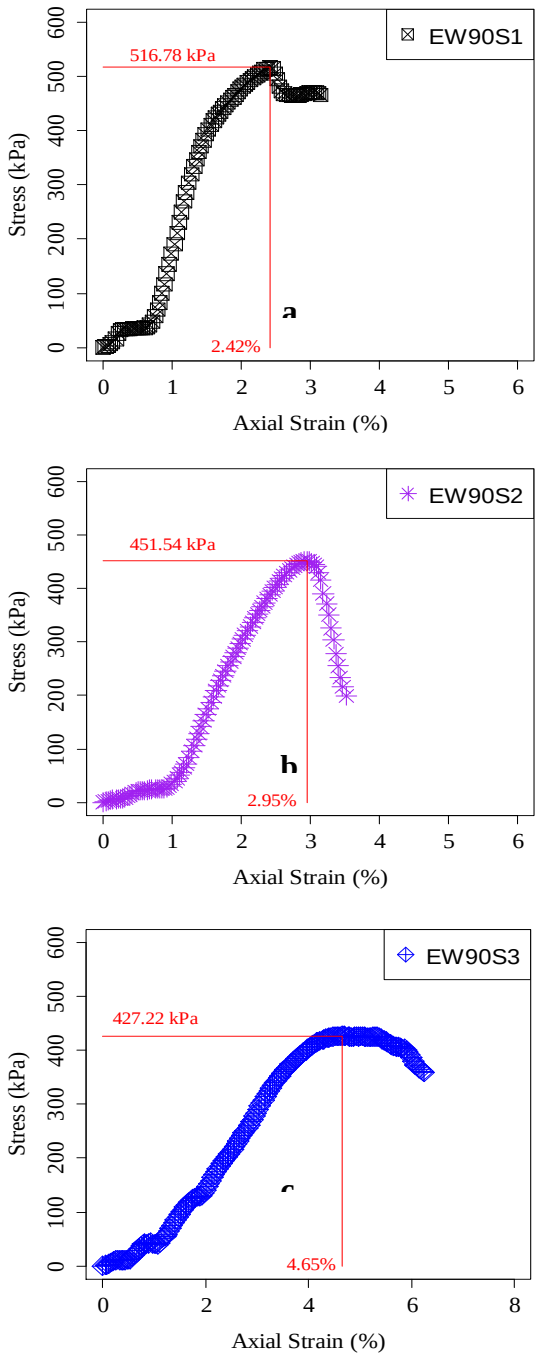

Figure 11. Stress-axial strain graphs for mixtures having 90% water content.

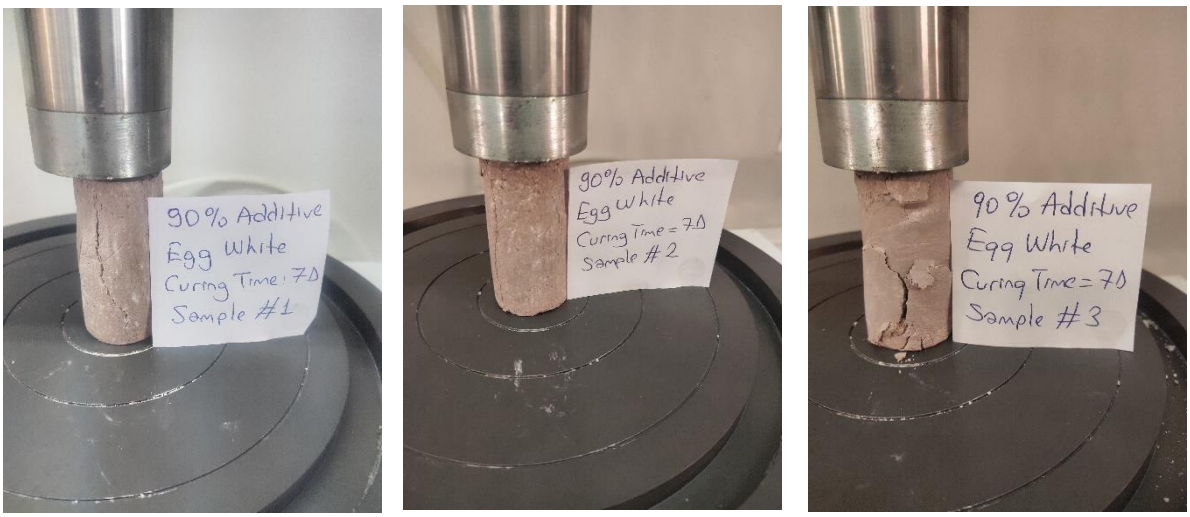

a) **b)** **c)**

Figure 12. Failure views for samples **a)** EW90S1 **b)** EW90S2 **c)** EW90S3.

The unconfined compression strength (UCS) of the EW100S1 sample is determined to be 412.14 kPa, with an ε value of 2.17% at the maximum stress, as depicted in Fig. 13a. During the initial 45 seconds of the test (ε = 0 – 0.75) for the EW100S1 sample, stress enhancement was relatively gradual, followed by a rapid increase between ε = 0.75% and 2.17%. The behavior of the graphs for the EW100S1, EW100S2, and EW100S3 samples appeared similar, as observed in Figs. 13a, 13b, and 13c. However, the graphs for EW100S3 exhibit a slightly more brittle behavior compared to EW100S1 and EW100S2. There is a significant stress reduction of 200 kPa within a small ε range (between 3.6% and 4%) after reaching the maximum stress for EW100S3. This reduction occurs more rapidly compared to EW100S1 and EW100S2, as indicated by their respective graphs. The axial strain (ε) values at the maximum stress exhibit slight variations between the samples, ranging from 2.17% to 4.05%. The difference between the maximum and minimum UCS values is 72.76 kPa, which is considered acceptable given that one value is only 1.18 times that of the other. The average UCS of the three samples is determined to be 442.51 kPa, which is close to the value of the second sample (EW100S2). Regarding failure behavior, EW100S1 and EW100S2 samples exhibit similar characteristics, with the breaking initiating from the bottom and displaying a comparable shape, as depicted in Figs. 14a and 14b. In contrast, EW100S3 demonstrates a typical failure behavior (Fig. 14c) when considering the axial stress-strain graph (Fig. 13c) in conjunction. A significant decrease in stress (approximately 180 kPa within an ε range between 3.60% and 4%) is observed after the occurrence of maximum stress.

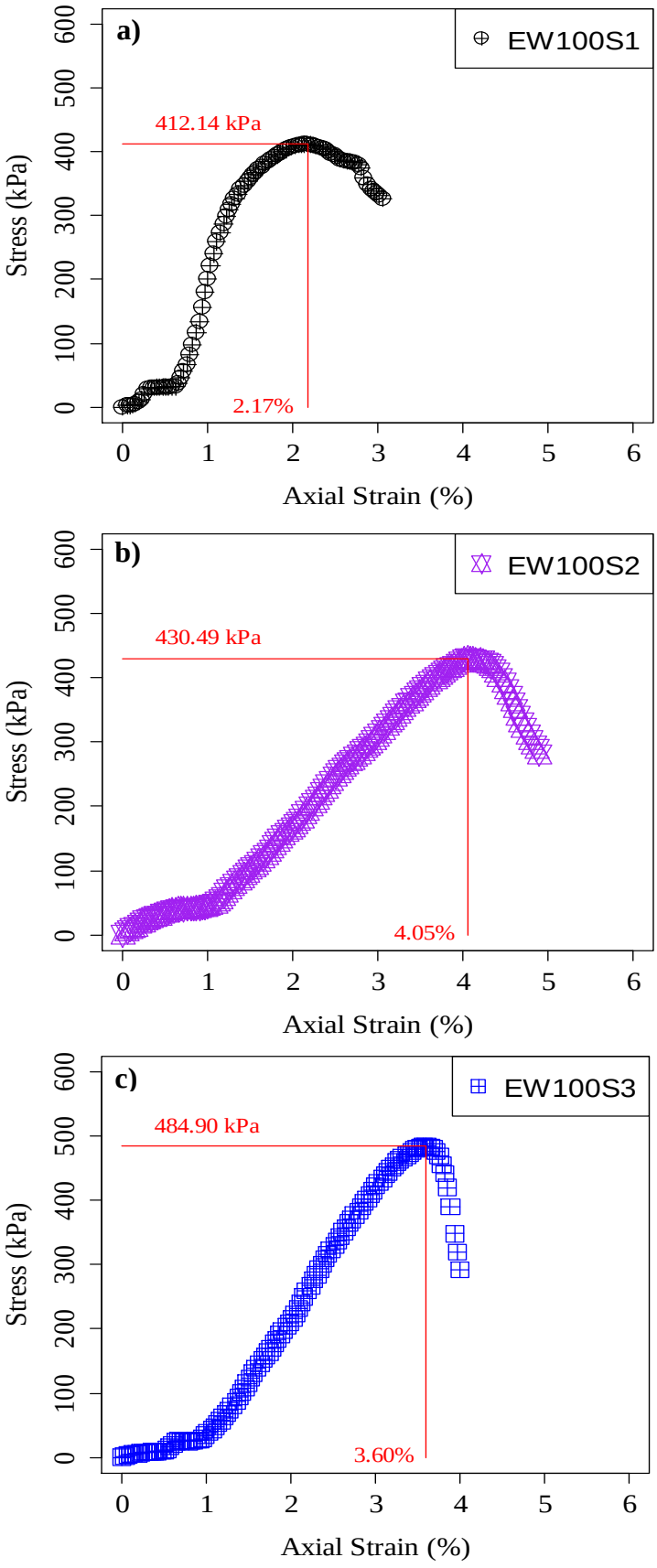

Figure 13. Stress-axial strain graphs for mixtures having 100% water content.

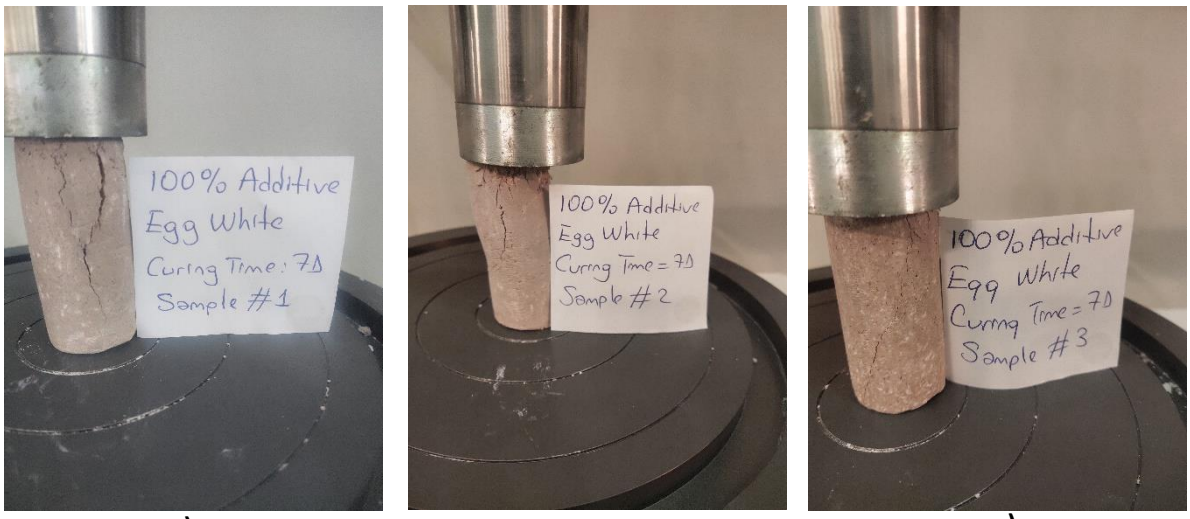

Figure 14. Failure views for samples **a)** EW100S1 **b)** EW100S2 **c)** EW100S3.

Table 3. Results of unconfined compression strength tests.

Mixture Code	Sample Number	ε (%)	UCS (kPa)
EW70S1	1	2.95	606.26
EW70S2	2	3.02	686.90
EW70S3	3	2.23	647.49
EW80S1	1	2.42	792.33
EW80S2	2	3.02	857.64
EW80S3	3	2.23	911.96
EW90S1	1	2.42	516.78
EW90S2	2	2.95	451.54
EW90S3	3	4.65	427.22
EW100S1	1	2.17	412.14
EW100S2	2	4.05	430.49
EW100S3	3	3.60	484.90

All the results have been compiled and presented in Table 3. It is noteworthy that the axial strain (ε) values corresponding to the attainment of UCS for the mixtures do not exceed 4.65%. The overall average of ε is calculated to be 2.98%. These strain values at maximum stress suggest that the mixtures have been effectively stabilized with lime. The increase in water content from 80% to 90% results in a significant reduction of approximately 45.43% in the average UCS value. Further increasing the water content up to 100% does not bring about any significant change in the UCS. The EW70 and EW80 samples exhibit ε values that do not surpass 3.02%, whereas the EW90 and EW100 samples demonstrate axial strains of 4.05% and 4.65% respectively. This observation may serve as an indication of the comparatively lower strength of the EW90 and EW100 samples when compared to the EW70 and EW80 samples.

4. Conclusion and Suggestions

In this study, the optimization of water content for Khorasan mortar samples was thoroughly investigated, leading to the following conclusions:

- The unconfined compression strength (UCS) test results revealed that mixtures containing 80% water content exhibited the highest UCS values, indicating their optimal composition.
- The samples with EW100 mixtures, which had the highest water content, exhibited the lowest UCS values. This suggests that increasing the water content beyond a certain threshold does not have a positive effect on the strength of the mixtures. On average, the UCS of these mixtures was approximately 0.518 times lower than that of the EW80 mixtures.
- Water contents lower than 70% were also experimented with, but the lack of sufficient moisture resulted in poor cohesion between particles. As a consequence, the samples were dry and prone to breakage upon extrusion from the sample extractor.
- These findings highlight the importance of considering the water content when preparing Khorasan mortar. Insufficient water content, without proper research, may be responsible for the lower unconfined compression strength observed in the samples.

These conclusions offer valuable insights for the preparation of Khorasan mortar, emphasizing the

significance of optimizing the water content to achieve the desired strength and quality in the mortar.

Acknowledgment

The authors wish to express their thanks to the authors of the literature for the supplied scientific aspects and ideas for this study.

Conflict of Interest Statement

There is no conflict of interest between the authors.

Statement of Research and Publication Ethics

The study is complied with research and publication ethics.

References

[1] M. S. Akman, A. Güner, and İ. H. Aksoy, "The history and properties of khorasan mortar and concrete," *II. Uluslararası Türk-İslam Bilim ve Teknoloji Tarihi Kongresi, İstanbul, Türkiye, April 28- May 2, 1986*, pp. 1-11.

[2] İ. Kılıç, "Horasan harcında yumurta akı kullanımının incelenmesi" *Kırklareli Üniversitesi Journal of Engineering and Science*, vol. 7-1, pp. 122-134, June 2021.

[3] T. İsafça-Kaya, K. Karakuzu, S. Özen, A. Mardani, and A. Doğangün, "Effects of shrinkage reducing admixture and polypropylene fiber utilization on some fresh state, mechanical and durability properties of khrosan mortar" *International Journal of Architectural Heritage*, July 2022, https://doi.org/10.1080/15583058.2022.2100295..

[4] H. S. Şengel, M. Canbaz, and E. Güler, "Utilization of ceramic waste in the production of Khorasan mortar" *Challenge Journal of Structural Mechanics*, vol. 5, no. 3, pp. 80-84, 2019, https://doi.org/10.20528/cjsmec.2019.03.001.

[5] N. Arıoğlu, and S. Acun, "A research about a method for restoration of traditional lime mortars and plasters: A staging system approach" *Building and Environment*, vol. 41, no. 9, pp. 1223-1230, September 2006, https://doi.org/10.1016/j.buildenv.2005.05.015.

[6] H. Böke, S. Akkurt, and B. İpekoğlu, "Tarihi yapılarda kullanılan horasan harcı ve sıvalarının özellikleri [The properties of Khorasan mortar and plasters used in historical buildings]" *Yapı Dergisi*, 2004.

[7] B. Işıkdağ, and İ. B. Topçu, "Improvement of Khorasan mortar with fly ash for restoration of historical buildings" *Science and Engineering of Composite Materials*, vol. 21, no. 3, pp. 359-367, 2014, https://doi.org/10.1515/secm-2013-0065.

[8] A. Bilal, "Investigation of hydraulic binding characteristics of lime based mortars used in historical masonry structures" *IOP Conf. Series: Materials Science and Engineering*, vol. 245, 022081, 2017, https://doi.org/10.1088/1757-899X/245/2/022081

[9] C. B. Emrullahoğlu Abi, and E. Abi, "Bentonite doped Khorasan mortar" *Academic Journal of Science*, vol. 08, no. 02, pp. 43-54, 2018.

[10] ASTM D2166/D2166M-16. Standard test method for unconfined compressive strength of cohesive soil, 2016. pp. 1-7.

[11] M. Canbaz and E. Güler, "The Effect of Lime Type on the Properties of Khorasan Mortar" *6th Symposium on Conservation and Strengthening of Historical Buildings*, Trabzon, 2017.